Journal of Coordination Chemistry

ISSN: 0095-8972 (Print) 1029-0389 (Online) Journal homepage: http://www.tandfonline.com/loi/gcoo20

[M{κ^2S,S-S_2C-piperazine-C_2H_4N=C(R)}$_n$] {Co(III), Ni(II), Cu(II) or Zn(II)} complexes bearing pendant Schiff base moieties: spectral characterization, fluorescence, cyclic voltammetric and TGA/DTA study

Sanjay K. Verma & Vinay K. Singh

To cite this article: Sanjay K. Verma & Vinay K. Singh (2015) [M{κ^2S,S-S_2C-piperazine-C_2H_4N=C(R)}$_n$] {Co(III), Ni(II), Cu(II) or Zn(II)} complexes bearing pendant Schiff base moieties: spectral characterization, fluorescence, cyclic voltammetric and TGA/DTA study, Journal of Coordination Chemistry, 68:6, 1072-1087, DOI: 10.1080/00958972.2014.1003550

To link to this article: http://dx.doi.org/10.1080/00958972.2014.1003550

Journal of Coordination Chemistry, 2015
Vol. 68, No. 6, 1072–1087, http://dx.doi.org/10.1080/00958972.2014.1003550

[M{κ^2*S*,*S*-S_2C-piperazine-C_2H_4N=C(R)}$_n$] {Co(III), Ni(II), Cu(II) or Zn(II)} complexes bearing pendant Schiff base moieties: spectral characterization, fluorescence, cyclic voltammetric and TGA/DTA study

SANJAY K. VERMA and VINAY K. SINGH*

Faculty of Science, Department of Chemistry, The Maharaja Sayajirao University of Baroda, Vadodara, India

(*Received 7 November 2014; accepted 18 December 2014*)

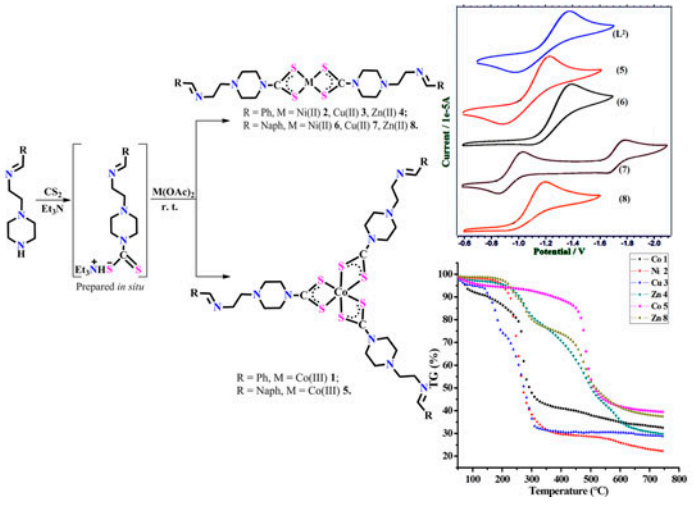

A series of neutral mononuclear complexes [M{κ^2*S*,*S*-S_2C-piperazine-C_2H_4N=C(R)}$_n$] {R = Ph; M = Co(III) **1**, Ni(II) **2**, Cu(II) **3**, Zn(II) **4**; R = Naph; M = Co(III) **5**, Ni(II) **6**, Cu(II) **7**, Zn(II) **8**; n = 2 for **2–4**, **6–8** and n = 3 for **1**, **5**} bearing pendant Schiff base moieties were synthesized through self-assembly involving N-[phenylmethylidene]-2-piperazin-1-ylethanamine (L^1) or N-[naphthylmethylidene]-2-piperazin-1-ylethanamine (L^2) with two equivalents each of CS_2 and corresponding metal acetates. The complexes **1–8** were characterized by microanalysis, ESI-MS, IR, ^{1}H, ^{13}C NMR, DEPT 135, UV–visible absorption, and emission spectroscopy. Complexes **1**, **3,** and **8** exhibit fluorescence emissions at 342, 344, and 348 nm upon excitation at 273 (for **1** and **3**) and 263 (for **8**) with concomitant Stokes shifts of 69, 71, and 85 nm. The spectral and magnetic moment data support octahedral geometry around Co(III) and square planar/tetrahedral geometry around other metal centers. Thermal stabilities of **1–8** have been investigated by thermogravimteric analysis. The cyclic voltammograms clearly suggest that the complexes exhibit electroreduction principally associated with pendant imine moieties except Cu(II) complex **7** which displays quasi-reversible reduction

*Corresponding author. Email: vinay.singh-chem@msubaroda.ac.in

corresponds to the Cu(II)/Cu(I) redox couples, in addition to reversible electroreduction of pendant imine groups associated with the coordinated ligands.

Keywords: Dithiocarbamate; Mononuclear complexes; Fluorescence; Cyclic voltammetric; TGA/DTA

1. Introduction

Transition metal complexes derived from sulfur-rich ligands exhibit a wide range of applications in electrical conductivity, molecular magnetism, electrochemical, biological processes, and optoelectronic properties [1]. Dithiocarbamates are of particular interest due to the ease of synthesis, ability to bind to transition elements supporting a wide range of oxidation states [2], and potential uses in medicine due to the existence of dithiocarbamate in a variety of biologically active molecules [3]. Many dithiocarbamate complexes have been used as single-source precursors for synthesis of high-quality semiconductor nanoparticles [4]. Thermogravimetric study of dithiocarbamate complexes supports industrial applications such as foam rubber, fungicides, effective heat stabilizers, antioxidant action, reprocessing of polymers [5] and as single-source precursors for the synthesis of metal sulfide nanoparticles and thin films [6]. The size and shape of the metal sulfide nanoparticles greatly depend on the nature of organic moiety present in metal dithiocarbamate complexes which affect fundamental properties such as optical, electrical, and mechanical [7].

While dithiocarbamate complexes containing simple alkyl/aryl substituents have been synthesized and their study is well documented in literature, functionalization of the backbone of these dithiocarbamate ligands is still in its early stage [8] and offers new applications and interactions viz. functionalization of gold nanoparticles [9], the synthesis of supramolecular systems which can be used for anion binding [10], the development of radiopharmaceuticals [11] and efficient chelators for the treatment of acute cadmium intoxication [12].

Reports have emerged on the applicability of piperazine derivatives; for instance, piperazinyl-linked ciprofloxacin dimers and other derivatives of piperazine are potent antibacterial agents against resistant strains, dual calcium antagonist, antimalarial agents, antifungal agents, and potential antipsychotic agents [13]. However, dithiocarbamate derivatives of functionalized piperazine and their transition metal complexes are far less studied [2(d)].

Thus, we undertake the synthesis of simple functionalized dithiocarbamate complexes based on N-[arylmethylidene]-2-piperazin-1-ylethanamine backbones bearing pendant Schiff base moieties. These complexes are thoroughly characterized by microanalysis, ESI-MS, FT-IR, ^{1}H and ^{13}C NMR, UV–visible absorption, fluorescence, thermogravimetric and cyclic voltammetric studies.

2. Experimental

2.1. *Materials and methods*

All solvents were purchased from commercial sources and freshly distilled prior to use. Reagents such as metal acetates $Co(OAc)_2{\cdot}4H_2O$, $Ni(OAc)_2{\cdot}4H_2O$, $Cu(OAc)_2{\cdot}H_2O$, and $Zn(OAc)_2{\cdot}2H_2O$ were purchased from Merck and used without purification. Microanalyses (C, H, N, and S) were carried out on a Perkin–Elmer 2400 analyzer. ESI-MS was obtained from an AB SCIEX, 3200 Q TRAP LC/MS/MS system. The MPs were recorded in open

capillaries and are uncorrected. FTIR (KBr pellets) spectra were recorded from 4000 to 400 cm^{-1} using a Perkin–Elmer spectrometer. ^{1}H and ^{13}C NMR spectra were recorded on a Bruker 400 MHz spectrometer in DMSO-d_6 unless otherwise noted. UV–visible absorption spectra were recorded on a Perkin–Elmer Lambda 35 UV–visible spectrophotometer, and fluorescence spectra were recorded on a JASCO spectrofluorometer model FP-6300. TGA/DTA plots were obtained using SII TG/DTA 6300 in flowing N_2 with a heating rate of 10 °C min^{-1}. Electrochemical measurements were performed on a CH Instruments 600C potentiostat using a Pt disk as the working electrode, Ag/AgCl as the reference electrode and a Pt wire as the counter electrode. Voltammograms were recorded using anhydrous solutions of the metal complexes in DMF (1.0 mM) containing tetra-n-butylammoniumhexafluoro phosphate (0.1 M) as supporting electrolyte.

2.2. *Synthesis*

2.2.1. Synthesis of N-[phenylmethylidene]-2-piperazin-1-ylethanamine, L^1. This ligand precursor has been synthesized by a modified literature procedure [13(c)] in 95% yield. To a solution of benzaldehyde (831 mg, 7.84 mM) in 25 mL of toluene containing 2–3 drops of glacial acetic acid was added 1-(2-aminoethyl)-piperazine (1000 mg, 7.74 mM) with rigorous stirring. The reaction mixture was refluxed for 2 h using a Dean–Stark apparatus. The progress of the reaction was monitored by TLC. The reaction mixture was cooled at room temperature, and solvent was evaporated under vacuum. The residue was dissolved in dichloromethane and washed with 5% aqueous sodium carbonate solution followed by distilled water 3–4 times. The dichloromethane layer containing crude product was separated and dried over sodium sulfate for 2 h. The solvent was evaporated under vacuum, and the product was purified by column chromatography using 3% methanol/chloroform (v/v) solution as eluent. The product (L^1) was stored under nitrogen, and samples were taken for analysis.

Mw: 217.3. Light yellow solid. Yield: 1597 mg (95%). IR (cm^{-1}): 3275 (N–H), 3061 (C-H), 1644 (C=N), 1449 (C=C). ^{1}H NMR (400 MHz, DMSO-d_6): 2.29 (s, 1H, N–H), 2.38–2.49 (t, 6H, CH_2), 2.51–2.55 (m, 2H, CH_2), 2.68–2.70 (t, 2H, CH_2), 3.60–3.69 (m, 2H, CH_2), 7.15–7.17 (t, 1H, *Ph*), 7.40–7.45 (m, 2H, *Ph*), 7.67–7.73 (m, 2H, *Ph*), 8.29 (d, 1H, HC=N). ^{13}C NMR (400 MHz, DMSO-d_6): δ 161.8 (d, 1C, HC=N), 136.6, 131.0, 129.1, 128.88, 128.25, 127.87 (all correspond to the carbons of *Ph*), 59.6, 58.6, 54.4, 53.6, 48.8, 45.8 (all correspond to the aliphatic carbons). DEPT 135 NMR (400 MHz, DMSO-d_6): δ 161.8 (HC=N), 131.0 (CH), 129.1 (CH), 128.88 (CH), 128.25 (CH), 127.87 (CH), 59.57 (CH_2), 58.66 (CH_2), 54.37 (CH_2), 53.67 (CH_2), 45.79 (CH_2).

2.2.2. Synthesis of N-[naphthylmethylidene]-2-piperazin-1-ylethanamine, L^2. To a solution of naphthaldehyde (1223 mg, 7.84 mM) in 25 mL of toluene containing 2–3 drops of glacial acetic acid was added 1-(2-aminoethyl)-piperazine (1000 mg, 7.74 mM) with rigorous stirring. The reaction mixture was refluxed for 2 h using a Dean–Stark apparatus. The progress of the reaction was monitored by TLC. The reaction mixture was cooled at room temperature, and solvent was evaporated under vacuum. The residue was dissolved in dichloromethane and washed with 5% aqueous sodium carbonate solution followed by distilled water 3–4 times. The dichloromethane layer containing crude product was separated and dried over sodium sulfate for 2 h. The solvent was evaporated under vacuum, and the

product was purified by column chromatography using 6% methanol/chloroform (v/v) solution as eluent. The product (L^2) was stored under nitrogen, and samples were taken for analysis.

Mw: 267.4. Light brown solid. Yield: 2155 mg (96%). IR (cm^{-1}): 3195 (N–H), 2996 (C-H), 1649 (C=N), 1503, 1456 (C=C). ^{1}H NMR (400 MHz, DMSO-d_6): δ 3.15 (s, 1H, N–H), 2.27 (s, 2H, CH_2), 2.49–2.51 (t, 2H, CH_2), 2.56–2.62 (t, 2H, CH_2), 2.68–2.70 (t, 2H, CH_2), 3.68–3.71 (t, 2H, CH_2), 3.77–3.80 (t, 2H, CH_2), 7.14–7.16 (m, 1H, *Ph*), 7.45–7.60 (m, 3H, *Ph*), 7.81–8.01 (m, 3H, *Ph*), 8.94 (d, 1H, HC=N). ^{13}C NMR (400 MHz, DMSO-d_6): *δ* 162.0 (HC=N), 137.7, 133.9, 131.7, 131.0, 129.3, 128.9, 128.2, 127.4, 126.6, 125.7 (all correspond to *naphthyl group*), 59.7, 58.9, 55.4, 54.6, 53.7, 45.9 (all correspond to aliphatic carbons). DEPT 135 NMR (400 MHz, DMSO-d_6): *δ* 162.0 (HC=N), 131.2 (CH), 129.3 (CH), 128.9 (CH), 128.6 (CH), 127.4 (CH), 126.5 (CH), 125.7 (CH), 59.5 (CH_2), 58.9 (CH_2), 55.4 (CH_2), 54.6 (CH_2), 53.4 (CH_2), 51.5 (CH_2).

2.2.3. General synthesis of [M{κ^{2}S,S-S_2C-piperazine-C_2H_4N=C(R)}$_n$], 1–8. In a typical procedure, N-[phenylmethylidene]-2-piperazin-1-ylethanamine (434.6 mg, 2.0 mM) or N-[naphthylmethylidene]-2-piperazin-1-ylethanamine (534.8 mg, 2.0 mM) and excess CS_2*ca* (0.5 mL, 8.32 mM) were added in 20 mL of Et_3 N solvent. The reaction mixture was allowed to stir for 1 h at room temperature, wherein a change in color from colorless to yellow was observed. To this mixture, $Co(OAc)_2{\cdot}4H_2O$ (168 mg, 0.66 mM), $Ni(OAc)_2{\cdot}4H_2O$ (248 mg, 1.0 mM), $Cu(OAc)_2{\cdot}H_2O$ (201 mg, 1.0 mM), or $Zn(OAc)_2{\cdot}2H_2O$ (220 mg, 1.0 mM) were added with rigorous stirring, and the reaction was allowed to continue for 6 h at room temperature. The residue was filtered in a glass-sintered crucible and washed several times with distilled water, followed by n-hexane and diethyl ether to yield **1–8** which were dried under vacuum and stored under nitrogen before samples were taken for analysis. This synthetic methodology is outlined in scheme 2.

2.2.3.1. *[Co{κ^{2}S,S-S_2C-piperazine-C_2H_4N=C(Ph)}$_3$] (1).* Mw: 936.2. Green solid. Yield: 549.9 mg (89%). M.p.: 245–250 (dec). Anal. Calcd for $C_{42}H_{54}N_9S_6Co$ (%): C, 53.88; H, 5.81; N, 13.46; S, 20.55. Found: C, 53.97; H, 5.71; N, 13.52; S, 20.63. IR (cm^{-1}): 2935 (C–H), 1636 (C=N), 1492 (N–CS_2), 1433 (C=C), 999 (C–S). NMR data could not be recorded due to poor solublility in DMSO even in acidic medium.

2.2.3.2. *[Ni{κ^{2}S,S-S_2C-piperazine-C_2H_4N=C(Ph)}$_2$] (2).* M.p.: 643.6. Green solid. Yield: 559.9 mg (87%). M.p.: 221–225 (dec). Anal. Calcd for $C_{28}H_{36}N_6S_4Ni$ (%): C, 52.25; H, 5.64; N, 13.06; S, 19.93. Found: C, 52.39; H, 5.71; N, 13.13; S, 20.01. IR (cm^{-1}): 3057 (C–H), 1639 (C=N), 1503 (N–CS_2), 1430s (C=C), 996 (C–S). ^{1}H NMR (400 MHz, DMSO-d_6 + D_2O + HCl ≈ 3 p^H): 3.2 (t, 2H, CH_2), 3.4 (t, 6H, CH_2), 3.5 (s, 4H, CH_2), 7.5–7.54 (t, 2H, *Ph*), 7.6 (d, 1H, *Ph*), 7.8 (d, 2H, *Ph*), 9.8 (d, 1H, HC=N). ^{13}C NMR (400 MHz, DMSO-d_6 + D_2O + HCl ≈ 3 p^H): *δ* 210.6 (–NCS_2), 194.6 (HC=N), 192.9, 135.3, 129.9, 129.6, 53.2, 48.8, 41.7, 34.5. DEPT 135 NMR (400 MHz, DMSO-d_6 + D_2O + HCl ≈ 3 p^H): *δ* 194.6 (HC=N), 135.3 (CH), 129.9 (CH), 129.6 (CH), 53.2 (CH_2), 48.8 (CH_2), 41.7 (CH_2), 34.4 (CH_2).

2.2.3.3. *[Cu{κ^{2}S,S-S_2C-piperazine-C_2H_4N=C(Ph)}$_2$] (3).* Mw: 648.4. Brown solid. Yield: 525.2 mg (81%). M.p.: 215–223 (dec). Anal. Calcd for $C_{28}H_{36}N_6S_4Cu$ (%): C, 51.86; H,

5.60; N, 12.96; S, 19.78. Found: C, 51.92; H, 5.75; N, 13.09; S, 19.86. IR (cm^{-1}): 2942 (C–H), 1642 (C=N), 1490s (N–CS_2), 1432s (C=C), 997 (C–S).

2.2.3.4. *[Zn{κ^2S,S-S_2C-piperazine-C_2H_4N=C(Ph)}$_2$] (4).* Mw: 650.3. White solid. Yield: 585.2 mg (90%). M.p.: 238–243 (dec). Anal. Calcd for $C_{28}H_{36}N_6S_4Zn$ (%): C, 51.72; H, 5.58; N, 12.92; S, 19.72. Found: C, 51.79; H, 5.64; N, 12.97; S, 19.79. IR (cm^{-1}): 2938 (C–H), 1643 (C=N), 1480s (N–CS_2), 1431s (C=C), 997 (C–S). ^{1}H NMR (400 MHz, DMSO-d_6): 3.36 (t, 6H, CH_2), 3.73 (t, 4H, CH_2), 4.0 (s, 2H, CH_2), 7.44–7.45 (t, 2H, *Ph*), 7.59–7.63 (t, 1H, *Ph*), 7.72–7.74 (dd, 1H, *Ph*), 7.90–7.92 (d, 1H, *Ph*), 8.36 (s, 1H, HC=N). ^{13}C NMR (400 MHz, DMSO-d_6): δ 193.6, 164.2, 135.0, 129.9, 129.6, 52.5, 51.2, 46.1. DEPT 135 NMR (400 MHz, DMSO-d_6): δ 164.4 (HC=N), 135.0 (CH), 129.9 (CH), 129.6 (CH), 52.5 (CH_2), 51.2 (CH_2), 47.5 (CH_2) 46.1 (CH_2). ESI-MS: *m/z* 651.1 $[M + H]^+$.

2.2.3.5. *[Co{κ^2S,S-S_2C-piperazine-C_2H_4N=C(Naph)}$_3$] (5).* Mw: 1086.4. Green solid. Yield: 602.3 mg (84%). M.p.: 265–271 (dec). Anal. Calcd for $C_{54}H_{60}N_9S_6Co$ (%): C, 59.70; H, 5.57; N, 11.60; S, 17.71. Found: C, 59.77; H, 5.63; N, 11.74; S, 17.85. IR (cm^{-1}): 2932 (C–H), 1640 (C=N), 1491s (N–CS_2), 1433s (C=C), 1003 (C–S). NMR could not be recorded due to poor solubility in DMSO even after acidification.

2.2.3.6. *[Ni{κ^2S,S-S_2C-piperazine-C_2H_4N=C(Naph)}$_2$] (6).* Mw: 743.7. Green solid. Yield: 639.5 mg (86%). M.p.: 230–234 (dec). Anal. Calcd for $C_{36}H_{40}N_6S_4$ Ni (%): C, 58.14; H, 5.42; N, 11.30; S, 17.25. Found: C, 58.23; H, 5.49; N, 11.38; S, 17.32. IR (cm^{-1}): 3043 (C–H), 1642 (C=N), 1509s (N–CS_2), 1437s (C=N), 994 (C–S). ESI-MS: *m/z* 745.0 $[M + H]^+$. NMR could not be recorded due to poor solubility in DMSO even after acidification.

2.2.3.7. *[Cu{κ^2S,S-S_2C-piperazine-C_2H_4N=C(Naph)}$_2$] (7).* Mw. 748.5. Brown solid. Yield: 621.2 mg (83%). M.p.: 205–212 (dec). Anal. Calcd for $C_{36}H_{40}N_6S_4Cu$ (%): C, 57.76; H, 5.39; N, 11.23; S, 17.13. Found: C, 57.82; H, 5.47; N, 11.30; S, 17.21. IR (cm^{-1}): 3049 (C–H), 1641 (C=N), 1486s (N–CS_2), 1432s (C=C), 995 (C–S).

2.2.3.8. *[Zn{κ^2S,S-S_2C-piperazine-C_2H_4N=C(Naph)}$_2$] (8).* Mw. 750.4. White solid. Yield: 675.3 mg (91%): M.p.: 208–217 (dec). Anal. Calcd for $C_{36}H_{40}N_6S_4Zn$ (%): C, 57.62; H, 5.37; N, 11.20; S, 17.09. Found: C, 57.75; H, 5.43; N, 11.35; S, 17.20. IR (cm^{-1}): 3047 (C–H), 1640 (C=N), 1474s (N–CS_2), 1429s (C=C), 998 (C–S). ^{1}H NMR (400 MHz, DMSO-d_6) (ppm): δ 2.62 (t, 8H, CH_2), 2.89 (t, 4H, CH_2), 3.56 (t, 4H, CH_2), 4.80 (m, 8H, CH_2), 7.58–7.64 (m, 4H, *Ph*), 7.67–7.77 (m, 2H, *Ph*), 7.91–7.93 (m, 2H, *Ph*), 7.98–8.08 (m, 4H, *Ph*), 8.20–8.22 (d, 1H, *Ph*), 8.29–8.31 (m, 1H, *Ph*), 9.03 (d, 1H, HC = N), 9.17 (d, 1H, HC = N). ^{13}C NMR (400 MHz, DMSO-d_6): δ 194.5, 166.4, 137.7, 136.0, 134.0, 129.3, 127.3, 125.8, 53.1, 51.1, 49.6, 46.1. DEPT 135 NMR (400 MHz, DMSO-d_6): δ 162.2 (HC=N), 135.5 (CH), 132.5 (CH), 131.0 (CH), 129.4 (CH), 127.6 (CH), 126.6 (CH), 125.9 (CH), 124.9 (CH), 123.4 (CH), 59.3 (CH_2), 58.1 (CH_2), 52.8 (CH_2), 51.0 (CH_2), 46.1 (CH_2).

3. Results and discussion

3.1. *Synthesis*

Condensation of 1-(2-aminoethyl)-piperazine with benzaldehyde or naphthaldehyde in toluene in acidic medium yielded the corresponding amine derivatives N-[phenylmethylidene]-2-piperazin-1-ylethanamine (L^1) and N-[naphthylmethylidene]-2-piperazin-1-ylethanamine (L^2) in good yields (scheme 1). The self-assembly process involving L^1 or L^2 with two equivalents each of CS_2 and corresponding metal acetates affords access to a new series of functionalized mononuclear dithiocarbamate complexes [$M\{\kappa^2 S,S$-S_2C-piperazine-$C_2H_4N{=}C(R)\}_n$] {R = Ph; M = Co(III) **1**, Ni(II) **2**, Cu(II) **3**, Zn(II) **4**; R = Naph; M = Co(III) **5**, Ni(II) **6**, Cu(II) **7**, Zn(II) **8**; n = 2 for **2–4**, **6–8** and n = 3 for **1**, **5**} bearing pendant Schiff

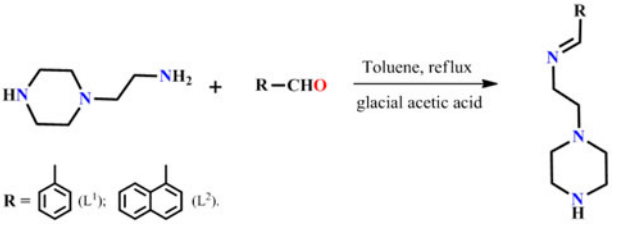

Scheme 1. Preparation of L^1 and L^2.

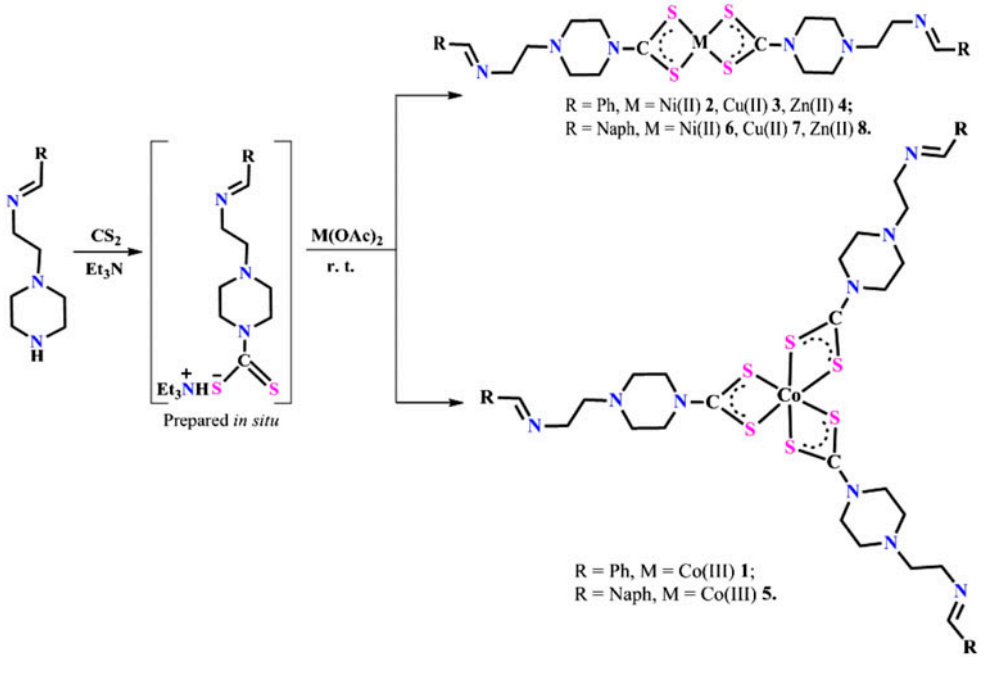

Scheme 2. Preparation of **1–8**.

base moieties (scheme 2). These complexes show moderate to poor solubility in common organic solvents and are stable in solid state and in solution over a period of days. The poor solubility of the majority of these complexes relates to the large number of intermolecular interactions. Our attempts to grow single crystals suitable for single crystal X-ray diffraction were unsuccessful. Similar complexes of heavy metals were previously derived [14] from piperazine derivatives such as *N*-[*β*-2,5-dimethyl-1-pyrrolyl)ethyl]piperazine and *N*-[*β*-salicylideneaminoethyl)]piperazine bearing protected amino groups. Professor Hogarth and his co-workers report that bis(dithiocarbamate) complexes with functionalized backbones can easily be prepared but their crystallization can be more problematic [15]. The precursors L^1, L^2 and mononuclear complexes were characterized by microanalysis and spectroscopy. The ESI-MS of **4** and **6** gave molecular ion peaks at *m/z* 651.1 and 745.0, respectively, which corresponds to $[M + H]^+$ along with differential fragmentation peaks (Supplementary material).

3.2. *IR spectral studies*

The characteristic IR bands for L^1, L^2 and mononuclear bis-dithiocarbamate complexes **1–8** are summarized in the Experimental section. A comparison of IR spectra of the complexes with L^1 and L^2 indicates that the υ(N–H) (3200–3300 cm^{-1}) seen for L^1 and L^2 (Supplementary material) disappears from IR spectra of **1–8** and two new sharp medium intensity bands at 1474–1509 cm^{-1} and 994–1003 cm^{-1} confirm bidentate coordination of dithiocarbamates [16]. These two regions are associated with ν(N–CS_2) and ν(S–C) stretching frequencies, respectively, and these are of particular interest in IR spectra of dithiocarbamate complexes. The values of ν(N–CS_2) (1474–1509 cm^{-1}) are between the range reported for C=N double bond (1650–1690 cm^{-1}) and C–N single bond (1250–1350 cm^{-1}), indicative of partial double bond character of N–CS_2 bonds, which would result in some partial double bond character for the C–S bonds. This is due to the mesomeric drift of an electron cloud of dithiocarbamate (–NCS_2) toward the metal ion. In addition to these new bands, all complexes exhibit bands at 3047–2932, 1649–1639, and 1509–1456 cm^{-1} due to υ(C–H), υ(C=N), and υ(C=C) stretches, respectively, which are associated with phenyl/naphthyl and imine of the ligand fragment in **1–8**. There is no significant change in the υ(C=N) band observed for the complexes compared to their precursors L^1 (1644 cm^{-1}) and L^2 (1649 cm^{-1}), which gives evidence for the presence of pendant Schiff base moieties in these complexes. The dithiocarbamato ligands generated *in situ* from L^1 and L^2 are monobasic bidentate in **1–8**.

3.3. *NMR spectral studies*

The ^{1}H NMR spectra of L^1 and L^2 display signals at δ 2.29, 3.15 ppm, and 8.33, 9.07 ppm, which are attributable to amine (–NH) and imine protons, whereas signals at 2.38–3.69 ppm and 7.15–7.73 ppm are associated with the aliphatic methylene and aromatic protons, respectively. The disappearance of amine signals and noticeable downfield shifting of aliphatic/aromatic NMR signals of **2**, **4**, and **8** compared to L^1 and L^2 (Supplementary material) confirm the involvement of these precursors in dithiocarbamate complex formation. The ^{13}C NMR spectra of **2** and **4** display downfield signals at 210.6 and 193.6 ppm, characteristic of coordinated dithiocarbamate (–NCS_2) [17]. In addition to the aliphatic and aromatic ^{13}C signals, these complexes further display signals at 194.6 and 161.5 ppm due to imine "–HC=N–"

carbons. A significant downfield shifting of the NMR signals (especially imine "–CH=N)" and dithiocarbamate ("–NCS_2") signals of **2** was observed when compared to similar signals of **4** and **8** whose spectra were taken in DMSO-d_6. The assignments of ^{13}C signals of L^1, L^2 and **2** are supported by DEPT 135 NMR spectral study which clearly distinguished the imine and aromatic carbons (in the positive region) from aliphatic methylene carbons (in negative region). No significant shift of imine (–CH=N) proton signals was observed in **4** and **8** compared to their positions in L^1 and L^2, and this rules out the possibility of involvement of Schiff base moieties in coordination.

3.4. *UV–visible absorption and magnetic moment studies*

The UV–visible absorption properties of L^1, L^2 and **1–8** were investigated at room temperature from 10^{-5} M DMSO solutions, and the pertinent results are summarized in table 1. The

Table 1. UV–visible and fluorescence spectral data of L^1, L^2 and **1–8** in 10^{-5} M DMSO solution.

Entry	λ_{max} nm (ε, L M^{-1} cm^{-1})	Wave number (cm^{-1})	Transitions	Magnetic moment μ_{eff} (BM)	Fluorescence spectral data	
					λ_{ex} (nm)	λ_{em} (nm)
L^1	260 (84,864)	38,461	$\pi\rightarrow\pi^*$	–	260	Non-fluorescent
L^2	288 (36,601)	34,722	$\pi\rightarrow\pi^*$	–	288	353(40) sh $\pi^*\rightarrow\pi$ 443(81) $\pi^*\rightarrow\pi$
1	273 (54,975)	36,630	$\pi\rightarrow\pi^*$	dia	273	301(68) sh $\pi^*\rightarrow\pi$
	325 (35,798)	30,769	$n\rightarrow\pi^*$			
	398 (16,231)	25,125	Charge transfer			342(225) $\pi^*\rightarrow\pi$
	635 (15,748)					
2	259 (52,283)	38,610	$\pi\rightarrow\pi^*$	dia	259	Non-fluorescent
	326 (69,905)	30,674	$n\rightarrow\pi^*$			
	388 (14,705)	25,773	Charge transfer			
3	273 (44,235)	36,630	$\pi\rightarrow\pi^*$	1.89	273	344(221) $\pi^*\rightarrow\pi$
	439 (16,231)	22,779	$n\rightarrow\pi^*$			
4	263 (66,853)	38,022	$\pi\rightarrow\pi^*$	dia	263	330(16) $\pi^*\rightarrow\pi$
	277 (56,501)	36,101	$n\rightarrow\pi^*$			
5	273 (55,376)	36,630	$\pi\rightarrow\pi^*$	dia	273	Non-fluorescent
	326 (36,182)	30,674	$n\rightarrow\pi^*$			
	395 (16,918)	25,316	Charge transfer			
	630 (15,873)					
6	259 (47,803)	38,610	$\pi\rightarrow\pi^*$	dia	259	Non-fluorescent
	325 (113,518)	30,769	$n\rightarrow\pi^*$			
	388 (21,838)	25,773	Charge transfer			
7	274 (75,967)	36,496	$\pi\rightarrow\pi^*$	1.95	274	Non-fluorescent
	437 (22,292)	22,883	$n\rightarrow\pi^*$			
8	263 (53,597)	38,022	$\pi\rightarrow\pi^*$	dia	263	348 (343) $\pi^*\rightarrow\pi$ 466 (266) $\pi^*\rightarrow\pi$
	278 (46,477)	35,971	$n\rightarrow\pi^*$			691 (151) $\pi^*\rightarrow\pi$

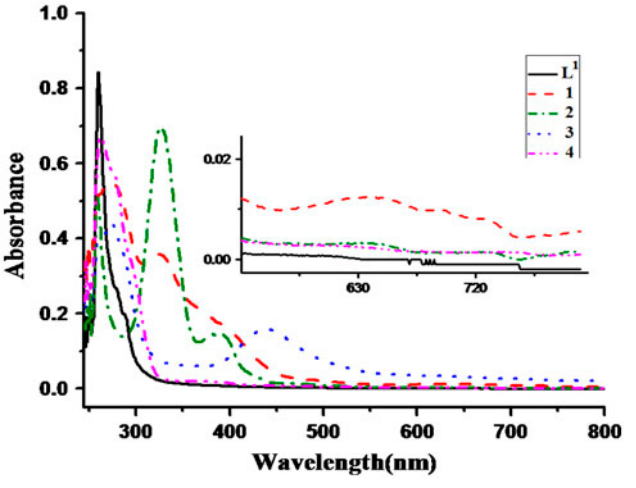

Figure 1. UV–visible absorption spectra of L^1 and mononuclear dithiocarbamate complexes at room temperature in 10^{-5} M DMSO solution.

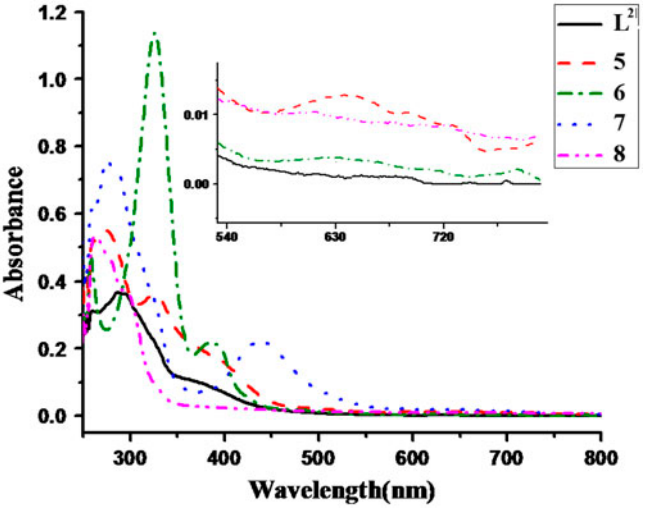

Figure 2. UV–visible absorption spectra of L^2 and mononuclear dithiocarbamate complexes at room temperature in 10^{-5} M DMSO solution.

assignment of UV–visible absorptions is based on literature reports on closely related compounds [18]. The UV–visible absorption spectra of the precursors and mononuclear complexes are shown in figures 1 and 2. L^1 and L^2 exhibit a single prominent band at shorter wavelength, 260 and 288 nm, respectively, assigned to $\pi \rightarrow \pi^*$ (phenyl) transitions [19]. All the dithiocarbamate complexes **1–8** exhibit maximum absorbance at 273, 259, 273, 263, 273, 259, 274, and 263 nm with the molar extinction coefficient values of 54,975, 52,283,

44,235, 66,853, 55,376, 47,803, 75,967, and 53,597, respectively, associated with the dithiocarbamate assigned to the N–C=S group. Bands at 325, 388, 439, 326, 388, and 437 nm observed for **1**, **2**, **3**, **5**, **6**, and **7**, respectively, are attributed to the ligand to metal charge transfer transition bands [18(e) and (f)]. In addition to these bands, Co(III) complexes **1** and **5** exhibit a weak absorption at ~630 nm, consistent with the absorption behavior of Co(III) tris-dipicolyldithiocarbamate complexes [18(g)]. The UV–visible absorption behavior of Cu(II) and Ni(II) complexes is quite similar to those obtained for bis(2-hydroxyethyl)dithiocarbamate complexes of these transition metals [18(h)]. The Zn(II) complexes **4** and **8** are diamagnetic and white with featureless electronic spectra presenting a broad absorption at ~263 nm. The magnetic moment values (table 1) along with UV–visible absorption bands suggest an octahedral environment around Co(III), square planar environment around Ni(II)/Cu(II), and tetrahedral environment around Zn(II) in their respective complexes.

3.5. *Fluorescence emission spectral studies*

The UV–visible emission properties of L^1, L^2 and **1–8** were investigated at room temperature (298 K) as 10^{-5} M DMSO solutions (table 1). The differential emission spectra of these compounds are shown in figure 3. L^2 exhibits fluorescence emissions at 353 and 443 nm upon excitation at λ_{max} = 288 nm, but we could not observe any noticeable fluorescence emission for L^1 upon excitation at 260 nm. Complexes **1**, **3**, and **8** exhibit maximum fluorescence emissions at 342, 344, and 348 nm upon excitation at 273 (for **1** and **3**) and 263 (for **8**) with concomitant Stokes shifts of ≈69, ≈71, and ≈85 nm. Copper(II) complexes are generally fluorescence quenchers; however, this copper(II) complex **3** shows very good fluorescence emission behavior upon excitation of the intraligand charge transfer band. A weak fluorescence emission at 330 nm with Stokes shift of 67 nm is observed for **4** upon excitation at 263 nm. Such a trend of fluorescence spectra and concomitant bathochromic shifts of intramolecular charge-transfer emissions by coordination compounds were previously

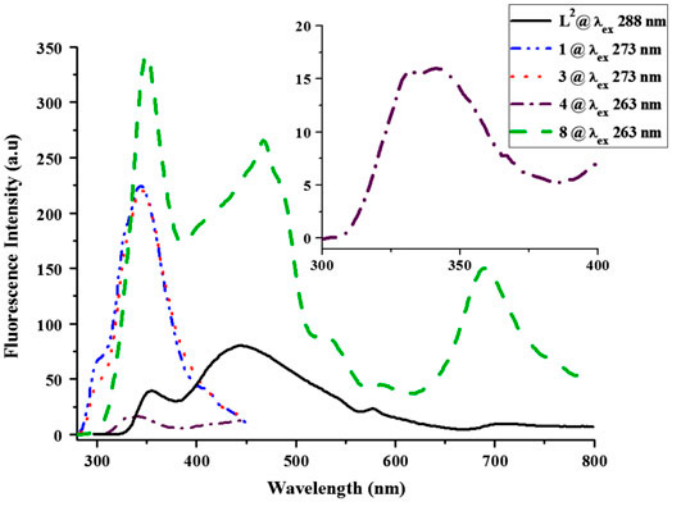

Figure 3. Fluorescence emission spectra of L^2 and mononuclear dithiocarbamate complexes at room temperature in 10^{-5} M DMSO solution.

observed in dithiocarbamate complexes [20], dialkoxo-bridged [21] and salen-type [22] complexes. The appearance of more bands upon excitation of a single wavelength (for L^2, **1** and **8**) as well as fluorescence behavior of the complexes may be attributed to reduction of photoinduced electron transfer on complex formation [23]. Emission spectra of **1**, **3**, and **8** showed similar patterns, that is, two or more kinds of fluorescence emission bands appear by excitation of single absorption band (in any case, shoulder is appearing). The complete quenching of fluorescence emissions is observed in **2** and **5–7**. The exact reason for the fluorescence quenching behavior of these complexes is not clear; however, literature reports suggest that fluorescence properties of the compounds depend on the molecular arrangements, achieved by means of polymorphism, conformational stiffness of the fluorophore (dihedral angles), intermolecular interactions such as $\pi\cdots\pi$ or C–H$\cdots\pi$ interactions, and upon the nature of substituents which can affect the photoinduced electron-transfer processes [24].

3.6. *Thermogravimetric studies*

Complexes **1–8** were studied for their thermal properties from room temperature to 750 °C. The heating rate was controlled at 10 °C min^{-1} – under an atmosphere of air. The mass losses over a range of temperature, rate of thermal decomposition, and the residual masses corresponding to final degradation products are summarized in table 2. The thermogravimetric plots (figure 4) suggest that **1** undergoes thermal degradation in two stages, whereas **5** exhibits single stage of mass loss and in both the cases mass loss, continues even at 750 °C. On the other hand, the thermal degradation of Ni(II) complexes **2** and **6**, essentially taking place in single stages, gives a broad peak on DTG curves. The TG curves clearly demonstrate that **2** decomposed completely with 77.3% of observed mass loss and a maximum rate of decomposition (0.299 mg min^{-1}) recorded at 250.7 °C on DTG curves. The stable residual mass obtained (22.7%) corresponds to $NiSO_4$ (Calcd 23.9%), whereas for **6**, the thermal degradation is incomplete and a continuous mass loss observed up to 750 °C. Interestingly, both **3** and **7** exhibit two stages of mass loss on DTG curves with a maximum rate of mass loss at 273.1 and 197.1 °C, respectively; both complexes give a stable residual

Table 2. Thermal analysis data of L^1, L^2 and **1–8**.

Entry	% Mass loss (temp. range °C)	DTG (°C) (mg min^{-1})	% Residue calculated (found)	Final product
1	5.9 (60–80) 61.22 (81–720) 67.12 (110–720)	70.0 (0.502), 270.5 (0.842)	– (32.88)	Incomplete degradation
2	77.3 (140–730)	250.7 (0.299)	23.9 (22.7)	$NiSO_4$
3	72.9 (141–400)	179.0 (0.129), 273.1 (0.168)	24.5 (27.1)	$CuSO_4$
4	77.2 (150–740)	158.6 (0.080), 261.1 (0.084), 316.2 (0.050)	24.7 (22.8)	$ZnSO_4$
5	65.2 (200–730)	256.9 (0.664)	– (34.8)	Incomplete degradation
6	63.4 (150–720)	262.1 (0.331)	– (36.6)	Incomplete degradation
7	77.0 (150–720)	197.1 (0.171), 261.0 (0.143)	21.2 (23.0)	$CuSO_4$
8	24.6 (120–200) 39.7 (201–450)	136.1 (0.072), 158.6 (0.087), 261.1 (0.106)	– (35.7)	Incomplete degradation

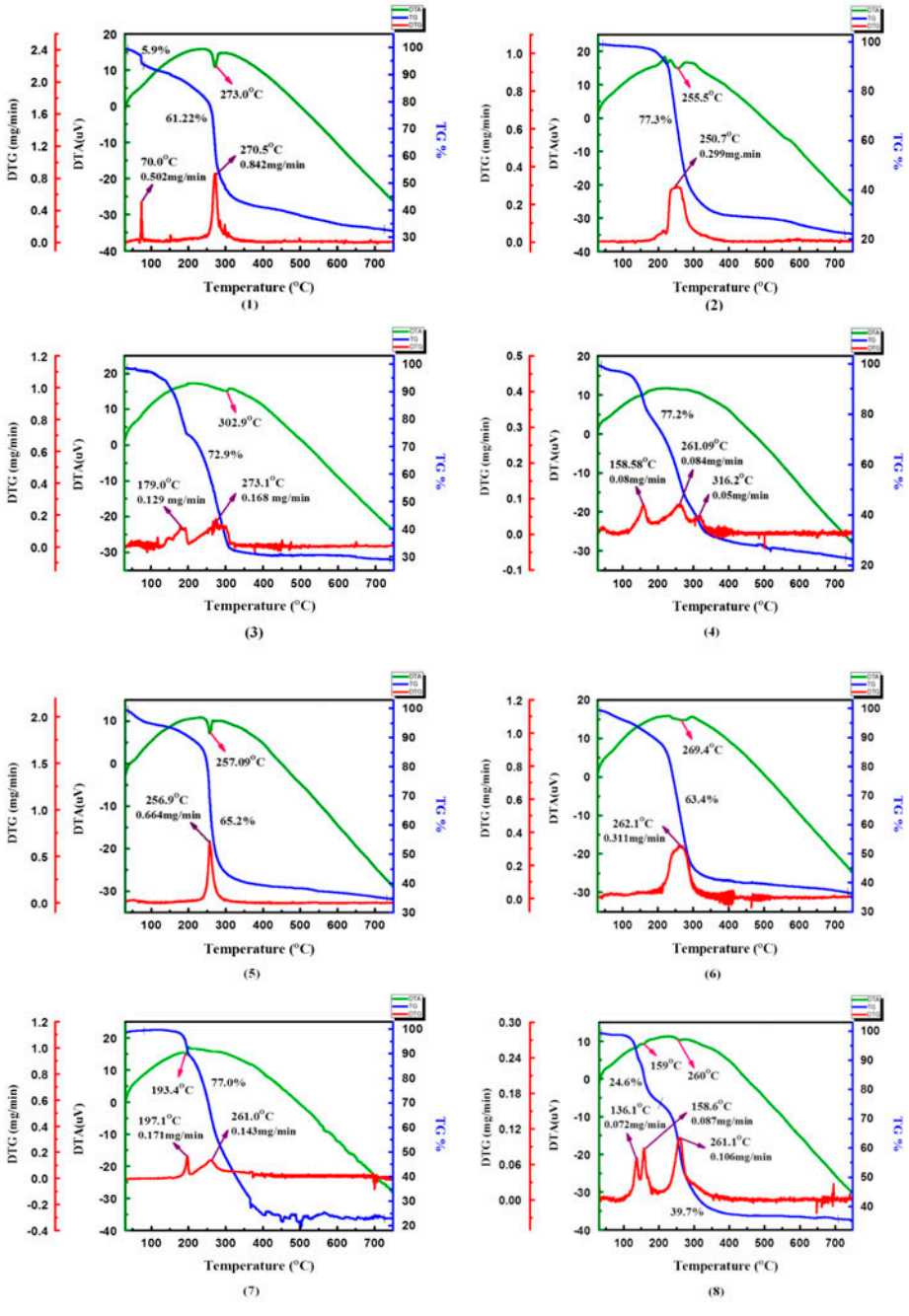

Figure 4. TG/DTA curves of N-[phenylmethylidene]-2-piperazin-1-ylethanamine (L^1), N-[naphthylmethylidene]-2-piperazin-1-ylethanamine (L^2) and complexes **1–8**.

mass of 27.1% and 23.0%, respectively, on TG curves, which corresponds to $CuSO_4$; however, both Zn(II) complexes **4** and **8** give three stages of degradation on DTG curves with

maximum rate of moss loss at 261.1 °C. TG curves reveal that the degradation of **4** is completed, giving a stable residual mass of 22.8% which corresponds to $ZnSO_4$ (Calcd 24.7), whereas only 64.3% of mass loss is observed for **8** up to 750 °C. Thermal decomposition of all the complexes starts before their melting point, and decompositions are accompanied by an endothermic peak on corresponding DTA curves. The formation MSO_4 as a stable residual product during the thermogravimetric analysis of transition metal dithiocarbamate complexes has been previously observed [25].

3.7. *Cyclic voltammetry*

The electrochemical behavior of L^2 and **5–8** in 1.0 mM DMF solutions was investigated from +2.0 to −2.1 V. The experiments were performed with a one-compartment cell having a platinum disk working electrode, a platinum wire counter electrode, and a Ag/Ag^+ (in acetonitrile) reference electrode. Voltammograms were recorded using anhydrous solutions of the metal complexes in DMF containing n-Bu_4NPF_6 (0.1 M) as supporting electrolyte at scan rate of 200 mV s^{-1}. The electrochemical examination of L^2 clearly demonstrates the reversible redox behavior in the potential range of −0.7 to −1.7 V. The

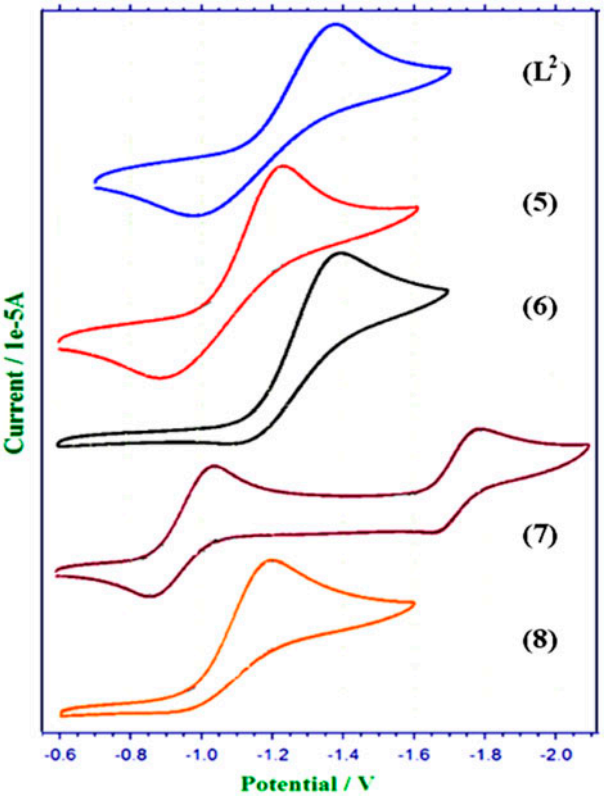

Figure 5. Cyclic voltammograms of a 1.0 mM solution of L^2 and **5–8** in DMF containing 0.1 M tetra-n-butylammonium hexafluorophosphate as the supporting electrolyte.

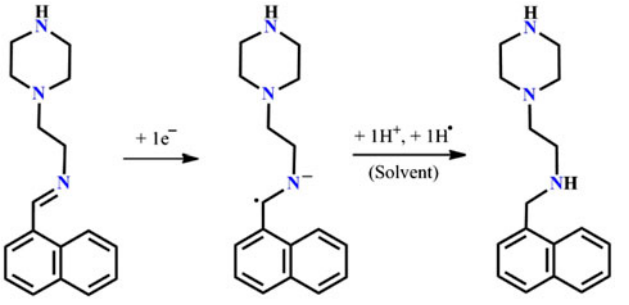

Scheme 3. Electroreduction of imine moiety.

constant value of peak potential separation ΔE_p and the peak current ratio ($I_{pa}/I_{pc} = 1$) at all scan rates at 25 °C in the analysis of L^2 is indicative of its reversible redox behavior. The reduction peak is at Epc = −1.375 in the cathodic scan of the cyclic voltammograms, which is apparently associated with the reduction of the imine (–N=C<) group as represented in scheme 3. The mono anion that is formed upon electroreduction of L^2 is protonated by the solvent to form an amino group which is confirmed by the fact that the reverse scans of the voltammograms show the anodic peak at Epa = −0.979 corresponding to oxidation of the amino group following the first cathodic peak of electroreduction of L^2. The electroreduction of imine (–N=C<) groups has been previously observed [26] in 1,2-bis[2-(pyridylmethylideneamino)phenylthio]ethanes and their transition metal complexes. The voltammograms of all the complexes (except **7**) examined in this work did not display any additional peak, compared to the cyclic voltammograms of L^2, in the cathodic or anodic scan under similar experimental conditions. This clearly demonstrates that these complexes are primarily electroactive with respect to the pendant imine (–N=C<) moieties of the coordinated ligands and the metal centers are silent. The cyclic voltammograms of the Ni(II) **6** and Zn(II) **8** displays a cathodic peak without corresponding anodic peak, and their cathodic peak potentials (Epc) were found to be −1.395 and −1.199 V, respectively, which are very close to the Epc of L^2. The Co(III) complex **5** displays reversible redox behavior, similar to that of L^2 with significantly greater values of I_{pc} and I_{pa} and slight anodic shift of Eps values associated with imine/amine redox couples, probably due to the presence of tris-dithiocarbamate coordinated ligands. Contrarily, the cyclic voltammogram of **7** displays additional peaks in the cathodic/anodic scans at less negative potentials (figure 5), apparently corresponding to the Cu^{II}/Cu^{I} redox couples. The separation between the anodic and cathodic peaks, DE = Epa − Epc, is 0.183 V which is larger than $\Delta E_p = 0.059/n$ V, and the ratio of the current intensity of the cathodic and anodic peaks is 1.65 which is different from unity. This clearly suggests a quasi-reversible process [27] essentially taking place at copper. The subsequent peaks which are significantly shifted to negative potential are associated with the reduction of the imine moiety of coordinated ligand. The increase in the electron density due to initial electroreduction of Cu(II) causes a significant cathodic shift of the electroreduction peaks associated with pendant imine moieties of coordinated dithiocarbamate in this complex.

4. Conclusion

A series of neutral mononuclear dithiocarbamate complexes of Co(III), Ni(II), Cu(II), and Zn(II) bearing pendant Schiff base moieties were efficiently synthesized through self-assembly involving the novel amine precursor N-[phenylmethylidene]-2-piperazin-1-ylethanamine (L^1) or N-[naphthylmethylidene]-2-piperazin-1-ylethanamine (L^2) with two equivalents each of CS_2 and corresponding metal acetates. The composition and structure of all complexes are well supported by physicochemical, spectroscopic data, and cyclic voltammetry. The thermogravimetric study performed on **1–8** indicates degradation starts before their melting points. Complexes **2**, **3**, **4**, and **7** degrade completely by 750 °C, giving a stable residual mass which corresponds to MSO_4. The IR, NMR, and cyclic voltammetric studies confirm the presence of pendant Schiff base moieties in all the complexes. Complexes **5**, **6**, and **8** are redox active only with respect to the ligand framework, whereas **7** is redox active with respect to the metal as well as coordinated ligands. Complex **7** displays a quasi-reversible reduction corresponding to the Cu(II)/Cu(I) redox couple in addition to reversible electroreduction of the coordinated ligands.

Supplementary material

The supplementary material for this paper is available online at http://dx.doi10.1080/00958972.2014.1003550.

Acknowledgements

VKS acknowledges CSIR, New Delhi for financial support (Project No. 01/(2733)/13/EMR-II), and SKV acknowledges the UGC for BSR-RFSMS fellowship.

References

[1] (a) D. Coucouvanis. *Prog. Inorg. Chem.*, **26**, 301 (1979); (b) E.R.T. Tiekink, I. Haiduc. *Prog. Inorg. Chem.*, **54**, 127 (2005); (c) M. Bousseau, L. Valade, J.P. Legros, P. Cassoux, M. Garbaukas, L.V. Interrante. *J. Am. Chem. Soc.*, **108**, 1908 (1986); (d) A.T. Coomber, D. Beljonne, R.H. Friend, J.L. Bredas, A. Charlton, N. Robertson, A.E. Underhill. *Nature*, **380**, 144 (1996); (e) N. Singh, V.K. Singh. *Transition Met. Chem.*, **26**, 435 (2001); (f) N. Singh, V.K. Singh. *Transition Met. Chem.*, **27**, 359 (2002); (g) A. Kobayashi, E. Fujiwara, H. Kobayashi. *Chem. Rev.*, **104**, 5243 (2004).

[2] (a) V. Singh, R. Chauhan, A.N. Gupta, V. Kumar, M.G.B. Drew, L. Bahadur, N. Singh. *Dalton Trans.*, **43**, 4752 (2014); (b) N. Singh, A. Kumar, R. Prasad, K.C. Molloy, M.F. Mahon. *Dalton Trans.*, **39**, 2667 (2010); (c) J.D.E.T. Wilton-Ely, D. Solanki, E.R. Knight, K.B. Holt, A.L. Thompson, G. Hogarth. *Inorg. Chem.*, **47**, 9642 (2008); (d) J.D.E.T. Wilton-Ely, D. Solanki, G. Hogarth. *Eur. J. Inorg. Chem.*, **4027**, (2005); (e) W.W.H. Wong, J. Cookson, E.A.L. Evans, E.J.L. McInnes, J. Wolowska, J.P. Maher, P. Bishop, P.D. Beer. *Chem. Commun.*, **2214**, (2005).

[3] (a) Y. Yoshikawa, Y. Adachi, H. Sukurai. *Life Sci.*, **80**, 759 (2007); (b) S. Ozkirimli, T.I. Apak, M. Kiraz, Y. Yegenoglu. *Arch. Pharm. Res.*, **28**, 1213 (2005); (c) V. Alverdi, L. Giovagnini, C. Marzamo, R. Seraglia, F. Bettio, S. Sitran, R. Graziani, D. Fregona. *J. Inorg. Biochem.*, **98**, 1117 (2004).

[4] (a) D. Fan, M. Afzaal, M.A. Mallik, C.Q. Nguyen, P.O. Brien, P.J. Thomas. *Coord. Chem. Rev.*, **251**, 1878 (2007); (b) W. Maneeprakorn, M.A. Mallik, P. O'Brien. *J. Mater. Chem.*, **20**, 2329 (2010); (c) N. Revaprasadu, M.A. Malik, P. O'Brien, G. Wakefield. *J. Mater. Res.*, **14**, 3237 (1999); (d) M.A. Malik, M. Motevalli, P. O'Brien. *Inorg. Chem.*, **34**, 6223 (1995); (e) M.A. Mallk, M. Motevalli, J.R. Walsh, P. O'Brien. *Organometallics*, **11**, 3136 (1992); (f) S. Mlowe, D.J. Lewis, M.A. Malik, J. Raftery, E.B. Mubofu, P. O'Brien, N. Revaprasadu. *New J. Chem.*, **38**, 6073 (2014).

[5] (a) A.K. Sharma. *Thermochim. Acta*, **104**, 339 (1986); (b) J.O. Hill, J.P. Murray, K.C. Patil. *Rev. Inorg. Chem*., **14**, 363 (1994).
[6] D.C. Onwudiwe, P.A. Ajibade. *Int. J. Mol. Sci.*, **12**, 1964 (2011).
[7] (a) A.A. Memon, M. Afzaal, M.A. Malik, C.Q. Nguyen, P. O'Brien, J. Raftery. *Dalton Trans*., 4499 (2006); (b) S. Senthilkumaar, R. Thamiz Selvi. *Synth. React. Inorg. Met.-Org. Nano-Met. Chem*., **38**, 710 (2008).
[8] C. Anastasiadis, G. Hogarth, J.D.E.T. Wilton-Ely. *Inorg. Chim. Acta*, **363**, 3222 (2010) and references cited therein.
[9] (a) J.D.E.T. Wilton-Ely. *Dalton Trans*., 25 (2007); (b) E.R. Knight, N.H. Leung, A.L. Thompson, G. Hogarth, J.D.E.T. Wilton-Ely. *Inorg. Chem*., **48**, 3866 (2009).
[10] J. Cookson, P.D. Beer. *Dalton Trans.*, 1459 (2007).
[11] P. Auzeloux, J. Papon, T. Masnada, M. Borel, M.F. Moreau, A. Veyre, R. Pasqualini, J.C. Madelmont. *J. Labelled Compd. Radiopharm.*, **42**, 325 (1999).
[12] (a) M.M. Jones, P.K. Singh, S.G. Jones, M.A. Holscher. *Pharmacol. Toxicol*., **68**, 115 (1991); (b) M.M. Jones, M.G. Cherian, P.K. Singh, M.A. Basinger, S.G. Jones. *Toxicol. Appl. Pharmacol*., **110**, 241 (1991).
[13] (a) P. Choudhary, R. Kumar, K. Verma. *Bioorg. Med. Chem*., **14**, 1819 (2006); (b) R.S. Upadhayaya, N. Sinha, S. Jain, N. Kishore, R. Chandra, S.K. Arora. *Bioorg. Med. Chem*., **12**, 2225 (2004); (c) S.G. Shingade, S.K.B. Bari. *Med. Chem. Res*., **22**, 699 (2013).
[14] R.N. Zagidullin. *Chem. Heterocycl. Compd.*, **25**, 1275 (1989).
[15] C. Anastasiadis, G. Hogarth, J.D.E.T. Wilton-Ely. *Inorg. Chim. Acta*, **363**, 3222 (2010).
[16] (a) S.M. Mamba, A.K. Mishra, B.B. Mamba, P.B. Njobeh, M.F. Dutton, E.F. Kankeu. *Spectrochim. Acta, Part A*, **77**, 579 (2010); (b) S.K. Verma, V.K. Singh. *Polyhedron*, **76**, 1 (2014).
[17] P. Valarmathi, S. Thirumaran, P. Ragi, S. Ciattini. *J. Coord. Chem.*, **64**, 4157 (2011).
[18] (a) B.S. Shyamala, P.V.A. Lakshmi, V.J. Raju. *J. Sci. Res*., **2**, 525 (2010); (b) P.C. Riveros, I.C. Perilla, A. Poveda, H.J. Keller, H. Pritzkow. *Polyhedron*, **19**, 2327 (2000); (c) B.F.G. Johnson, K.H. Al-Obaidi, J.A. McCleverty. *J. Chem. Soc. A*, 1668 (1969); (d) R.J. Anderson, D.J. Bendell, P.W. Groundwater, *Organic Spectroscopic Analysis*, RSC, Cambridge (2004); (e) W.W.H. Wong, D.E. Phipps, P.D. Beer. *Polyhedron*, **23**, 2821 (2004); (f) A. Gölcü, P. Yavuz. *Russ. J. Coord. Chem*., **34**, 106 (2008); (g) K. Vanthoeun, H. Yamazaki, T. Suzuki, M. Kita. *J. Coord. Chem*., **66**, 2378 (2013); (h) J.N. King, J.S. Fritz. *Anal. Chem*., **59**, 703 (1987).
[19] R. Kadu, V.K. Singh, S.K. Verma, P. Raghavaiah, M.M. Shaikh. *J. Mol. Struct.*, **1033**, 298 (2013).
[20] S.K. Verma, R. Kadu, V.K. Singh. *Synth. React. Inorg. Met.-Org. Nano-Met. Chem.*, **44**, 441 (2014).
[21] L.-Q. Chai, G. Wang, Y.-X. Sun, W.-K. Dong, L. Zhao, X.-H. Gao. *J. Coord. Chem.*, **65**, 1621 (2012).
[22] R. Pandey, P. Kumar, A.K. Singh, M. Shahid, P.Z. Li, S.K. Singh, Q. Xu, A. Misra, D.S. Pandey. *Inorg. Chem.*, **50**, 3189 (2011).
[23] S. Sreedaran, K.S. Bharathi, A.K. Rahiman, L. Jagadish, V. Kaviyarasan, V. Narayanan. *Polyhedron*, **27**, 2931 (2008).
[24] (a) Y. Mizobe, T. Hinoue, A. Yamamoto, I. Hisaki, M. Miyata,Y. Hasegawa, N. Tohnai. *Chem. Eur. J*., **15**, 8175 (2009) and references cited therein; (b) K.-H. Lee, C.-S. Choi, K.-S. Jeon. *J. Photosci*., **9**, 71 (2002); (c) S.C. Martens, U. Zschieschang, H. Wadepohl, H. Klauk, L.H. Gade. *Chem. Eur. J*., **18**, 3498 (2012); (d) A.C. Valdés, G. Pina-Luis, I.A. Rivero. *J. Mex. Chem. Soc*., **51**, 87 (2007); (e) D. Madrigal, G. Pina-Luis, I.A. Rivero. *J. Mex. Chem. Soc*., **50**, 175 (2006).
[25] B.F. Ali, W.S. Al-Akramawi, K.H. Al-Obaidi, A.H.A. Al-Karboli. *Thermochim. Acta*, **419**, 39 (2004).
[26] E.K. Beloglazkina, A.G. Majouga, A.A. Moiseeva, I.V. Yudin, F.S. Moiseev, O.I. Shmatova, N.V. Zyk. *Russ. Chem. Bull., Int. Ed*., **57**, 358 (2008).
[27] E. Lamour, S. Routier, J.-L. Bernier, J.-P. Catteau, C. Bailly, H. Vezin. *J. Am. Chem. Soc.*, **121**, 1862 (1999).